Turkish Journal of Physics

http://journals.tubitak.gov.tr/physics/

Research Article

Turk J Phys
(2017) 41: 507 – 519

doi:10.3906/fiz-1705-10

Temperature measurements in a manufactured RF plasma jet in various Ar/N_2 mixtures

Mohammad Nasir ROSTAMI RAVARI[1], Alireza GANJOVI[2,*], Farideh SHOJAEI[1], Amir FALAHAT[1]

[1]Faculty of Physics, Shahid Bahonar University of Kerman, Kerman, Iran
[2]Photonics Research Institute, Graduate University of Advanced Technology, Kerman, Iran

Received: 13.05.2017 • **Accepted/Published Online:** 14.08.2017 • **Final Version:** 18.12.2017

Abstract: In this paper, using the optical emission spectroscopy technique, a comparative study is performed on the argon excitation and nitrogen vibrational temperatures in the plasma discharge medium of a manufactured RF plasma jet. The argon contribution in the Ar/N_2 mixture is varied from 70% to 98% and the obtained optical emission spectra from argon and molecular nitrogen are analyzed. The highest emission intensities of neutral argon (Ar I) are recorded in the wavelength range of 790–850 nm. It is seen that, at the higher argon percentages in the mixture, the emission intensity from all the formed species in the plasma discharge medium of the RF plasma jet will increase. In addition, at the lower Ar contributions in the mixture, both the argon excitation and nitrogen vibrational temperatures are higher. Furthermore, it is shown that, at the higher Ar percentages in the mixture, both of the electronic temperatures are decreased.

Key words: RF plasma jet, optical emission spectroscopy, Ar/N_2 mixture

1. Introduction

Ar/N_2 mixture discharge plasma jets are being widely used in different fields of medical applications. These mainly include skin regeneration owing to the painless effects, wound healing, and sterilization and decontamination of medical instruments [1]. On the other hand, owing to the various applications of plasma jets with different power sources and active species produced from argon and nitrogen, using argon as the main carrier gas could give more interesting insights into RF plasma jets. Furthermore, since the existing resources for helium gas production are limited, argon is cheaper than helium gas [2].

In biomedical applications, the damaging effects of plasma jets on human body tissues must be insignificant. Thus, the charged particles' temperature in plasma discharge media should be kept relatively small. Fortunately, the electrons' temperature in the formed plasma discharge from the Ar/N_2 gaseous mixture in the RF plasma jet is about 1–4 eV. However, in such plasma discharge media, the background gas temperature remains at about room temperature. Thus, RF plasma jet devices have to lose heat properly and hence the applied power is reduced [3].

Qayyum et al. [4] reported the optical emission spectroscopic (OES) features of an Ar/N_2 gaseous plasma mixture with 50 Hz of pulsing-DC power in a parallel plate electrodes configuration. The input power was varied between 175 and 225 W and the filling pressure was kept between 7 and 9 mbar. Their findings showed that the

*Correspondence: ganjovi@kgut.ac.ir

intensity of molecular nitrogen emission lines and plasma temperature increased at higher argon percentages in the Ar/N_2 mixture.

Doronin et al. [5] analyzed the luminescence spectroscopic features of a supersonic jet with nitrogen clusters (containing nearly 100 molecules per cluster) and Ar/N_2 clusters (250 and 400 particles per cluster). For the Ar/N_2 clusters, the main transitions to the different vibrational levels of the ground state from single N_2 molecules in the argon medium were detected. Furthermore, it was observed that the emission lines of nitrogen atomic ions lay between the wavelengths of 140 and 220 nm.

The significant features of the atmospheric RF plasma jets mainly include the low gas temperature, controllability, production of plentiful reactive species, rapid mutation, and high operation flexibility [6]. Interestingly, in RF plasma jets, the plasma discharge is generally formed on the tip of an inner small diameter electrode. Thus, a stable RF plasma plume with small dimensions can be generated. Furthermore, the activation process of RF plasma jets is much easier compared with the other developed plasma jets. Thus, such a system can be easily installed in medical centers. Besides, while the processing temperature for RF plasma jets is very low, the system is safe and efficient. It is worth mentioning that the processing time is much shorter compared with the other existing systems for sterilization applications. Hence, it is suitable for the sterilization of living and nonliving tissues.

Generally, the OES technique is used to diagnose the reactive species in different plasma discharge media, where the other measurement techniques are impractical. Owing to the noninvasive character of its measurements, it can monitor the variations of the plasma species' densities in real time. Thus, in this paper, the OES technique is used as an emissive spectroscopy technique to measure the argon excitation and nitrogen vibrational temperatures in the plasma discharge medium of a RF dielectric barrier discharge (DBD) plasma jet working with an Ar/N_2 mixture. Moreover, the amount of Ar in the Ar/N_2 mixture is varied and an analytical study is performed on the obtained optical emission spectra from the atomic argon and molecular nitrogen in the plasma discharge medium of the jet.

2. Experimental setup

The schematic representations of the experimental setup with a typical view of the RF plasma jet, gas mixer, and spectrometer are shown in Figure 1a. For the designed RF plasma jet, both the central tungsten pin (inner) and aluminum shell (outer) electrodes are connected to a RF voltage power source. The inner electrode is made of a tungsten rod with the diameter and length of 1.6 mm and 95 mm, respectively. The outer electrode is made of an aluminum shell with the inner and outer diameter of 12 mm and 20 mm, respectively. Moreover, to provide the cold DBD plasma discharge between the inner and outer electrodes, the outer electrode is covered by a quartz tube. The inner and outer diameters of quartz tube are 4 mm and 6 mm, respectively. This RF plasma jet device is able to operate at atmospheric pressures in various Ar/N_2 mixtures. Thus, the plasma discharge is formed in a 1.2-mm gap between the inner electrode and quartz tube. In the operational conditions, sometimes the formed plasma length reaches about 20 mm. This arrangement for the RF plasma jet strongly prevents arcing between the inner and outer electrodes, which is particularly unwanted for the biomedical applications of plasma jets. It must be noted that such a configuration for the RF plasma jet generates a stable plasma discharge. The produced plasma transfers the reactive species to the processing region (plasma jet plume), which avoids disturbance of the plasma stability. Such a cold RF DBD plasma is suitable for technological applications such as biology, materials processing, and medicine. Moreover, this system has unique features in plasma medicine, such as wound sterilization or surgical and blood coagulation [7].

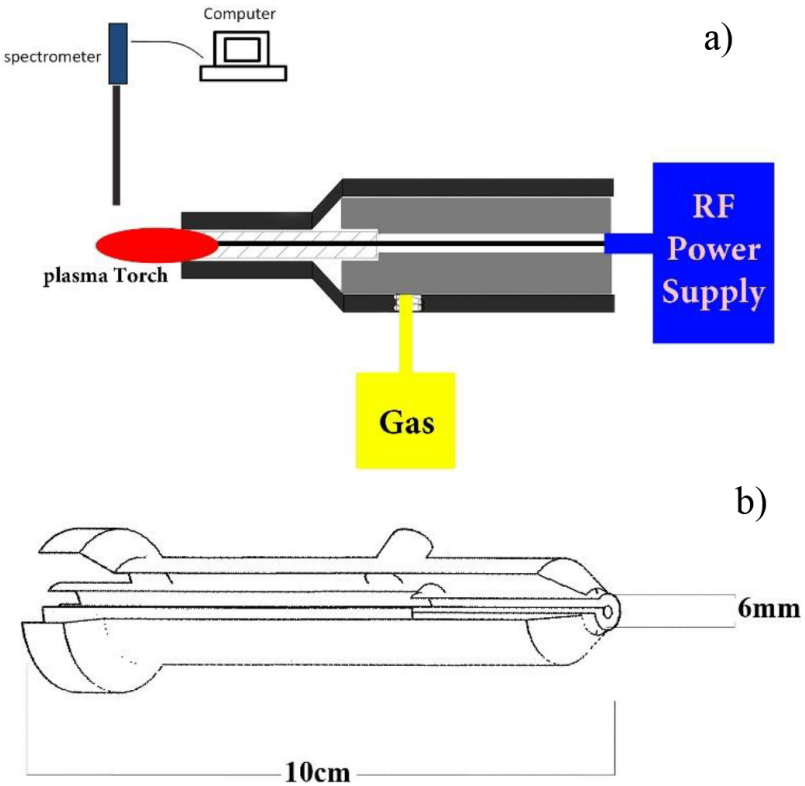

Figure 1. a) The experimental setup with typical view of the developed RF plasma jet, gas mixer, and spectrometer with 2D interior view of the RF plasma jet; b) 3D interior view of the developed RF plasma jet.

In this work, an RFG01BF Basafan power supply with a fixed RF frequency (13.56 MHz) and variable output power from 1 W to 100 W is used. The OES method is carried out using a USB2000+ spectrometer with the SpectraSuite software to analyze the obtained spectra. It has a linear CCD and spectral resolution of 0.35 nm as the FWHM and wavelength sensitivity range of 200–1100 nm. Argon is taken as the main carrier gas and it is mixed at different percentages with the molecular nitrogen using a gas mixer. The output gas from the gas mixture is injected to the RF plasma jet at a gas flow rate of about 15 standard liters per minute, which is controlled by a velocity flow controller. The output power was set as 48 W through an impedance matching network. The impedance matching network works based on transmission line matching using a lumped L-type network. It has to be noted that the L-type matching network is lossless or, at least, the loss can be potentially made small with the proper component choices. However, the RF input power depends on the application and the dimensions of the designed RF plasma jet. The experimental discharge structure and the measurement instrumentations are shown in Figure 1a. Using a 50-Ω coaxial cable and a matching network system, the RF power was coupled with the plasma jet.

It must be noted that this RF plasma jet is able to move easily and freely in all spatial directions. This is due to its very small dimensions and low weight compared with the RF plasma jets manufactured by Babayan et al. [8] and Weltman et al. [9]. Moreover, as shown in Figure 1b, its nozzle design focuses the plasma as a needle. This design is certainly more efficient in local medical treatments and the surrounding tissues will not be damaged. Thus, these features introduce such a RF plasma jet as a reliable tool in different medical and industrial applications. Moreover, a photograph of the RF plasma jet in working conditions is shown in Figure 2. It appears uniform to the human eye and its length can reach more than 20 mm.

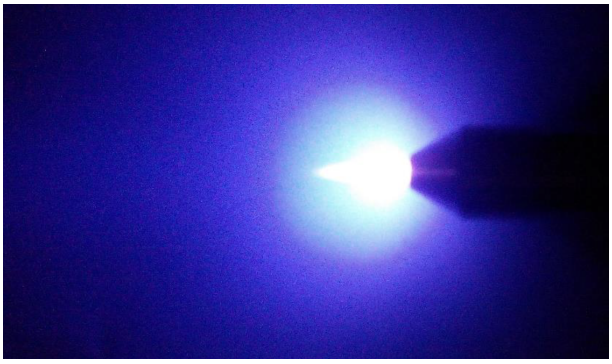

Figure 2. Photograph of the developed RF plasma jet in the operational conditions.

In this work, using the OES technique, the temperature of different formed species in the plasma discharge medium of a RF plasma jet and the population density of atomic and molecular states are estimated. Here, the experimental relative emission intensities of different lines originating from the gaseous atomic and molecular levels are measured. The amount of argon in the Ar/N_2 mixture is varied from 70% to 98%. The spectrometer is kept 1 cm away from the needle of the RF plasma jet. The obtained spectra from the formed plasma in the RF plasma jet are analyzed by SpectraSuite software. The obtained results from the OES technique are used to calculate the plasma discharge characteristics of the RF plasma jet such as average electron excitation temperature and vibrational temperature for the nitrogen molecules. In order to measure the discharge parameters of the RF plasma jet, the intensity of atomic emission lines of the plasma discharge is used to estimate the population in the electronic levels of the argon atoms. To this end, the Boltzmann distribution for plasma discharge in the RF plasma jet is taken into account.

The emission lines from the excited argon and nitrogen species are the most abundant, and these states have reliable transition probability values published in the existing literature. Assuming that the upper levels of the selected atomic transitions are in the partial local thermodynamics equilibrium conditions, the conventional Boltzmann plot technique can be used to determine the excitation temperature in the discharge medium of the designed RF plasma jet. Hence, the following relation expresses the relative transition probabilities of two different emission lines [10]:

$$\ln(\frac{I\lambda_{ki}}{A_{ki}g_k}) = \ln(\frac{hcN_0}{4\pi U(\mathrm{T})}) - \frac{E_k}{kT_{exc}}, \tag{1}$$

where I denotes the total intensity, A_{ki} is the transition probability, g_k is the degeneracy of the upper level, λ_{ki} is the wavelength, E_k is the excitation energy, and k is the Boltzmann constant. In this model, it is assumed that the electron collisions between excited atoms are dominant in the populating and depopulating of the excited atoms. From Eq. (1), a straight line fit for $\mathrm{Ln}(I\lambda_{ki}/A_{ki}g_k)$ as a function of E_k can be obtained. Consequently, the inverse of the absolute value of the well-fitted line slope is the electron excitation temperature (T_{exc}). Moreover, the NIST atomic database (Table 1) is used to plot Eq. (1).

Generally, the vibrational temperature of N_2 is determined through the second positive system of a nitrogen emission spectrum [11]. This implies the radiation transition between C and B electronic state as $N_2(C^3\Pi_u) \rightarrow N_2(B^3\Pi_g)$ [12]. Thus, the vibrational temperature, T_v, can be obtained using the following relation:

$$I(C, \nu' - B, \nu'') = c(\lambda).[N_2(C, \nu')].A(C, \nu' - B, \nu'')/\lambda, \tag{2}$$

where I(C, ν' – B, ν'') is the transition emission intensity between the two energy levels with the vibrational

Table 1. Several spectral parameters of the observed emission lines for Ar/N_2 gaseous mixture plasma discharge.

Ion	Wavelength (nm)	$A_{ki} \times 10^7$ (s^{-1})	E_i (eV)	E_k (eV)	Transition	G
Ar I	794.8176	1.86	11.7230789	13.2825466	4p-4s	3
	801.4786	0.92	11.54827415	13.0947815	4p-4s	5
	811.5311	3.31	11.54827415	13.0756248	4p-4s	7
	826.4522	1.53	11.82798894	13.3277644	4p-4s	3
	842.4648	2.15	11.62351193	13.0947815	4p-4s	5
	852.1442	1.39	11.82798894	13.2825466	4p-4s	3
Ion	Wavelength (nm)	$A_{ki} \times 10^7$ (s^{-1})	$\Delta\upsilon$	$\acute{\upsilon}$	Transition	Band
N_2	370.9	0.404	–2	2	$C^3\Pi_u \rightarrow B^3\Pi_g$	2nd positive system
	375.4	0.493	–2	1	$C^3\Pi_u \rightarrow B^3\Pi_g$	2nd positive system
	380.4	0.356	–2	0	$C^3\Pi_u \rightarrow B^3\Pi_g$	2nd positive system

numbers of ν' and ν''. In this method, $\Delta v = (v' - v'') = -2$. The function $c(\lambda)$ is the spectrometer response factor at the wavelength of λ, $[N_2(C, \nu')]$ is the density of nitrogen molecules in the C-state at level ν', and $A(C, \nu' - B, \nu'')$ is the spontaneous emission probability. Moreover, the density of nitrogen molecules can be expressed as $[N_2(C, \nu')] \approx I(C, \nu' - B, \nu'').\lambda/A(C, \nu' - B, \nu'')$ [11]. Finally, the vibrational temperature can be obtained as follows [13]:

$$N_2(\upsilon) = N_2(0)\exp[-hcG(\upsilon)/kT_v)]. \tag{3}$$

At low vibrational levels, including most of the vibrational excited molecules, a linear function versus ν can be obtained by taking the logarithm of Eq. (3) [14]. The vibrational temperature, T_v, is determined from the slope of the semilogarithmically plotted population density $(N_2(\nu_1)/N_2(\nu_2))$ versus vibrational quantum number ν [14].

On the other hand, the vibrational temperature of N_2 is calculated using the following relation [13]:

$$I_{\nu',\nu''} = const.\nu^4 A(\nu'\nu'')e^{\frac{E'_\nu}{k_B T}} I_{\nu',\nu''} = const.\nu 4A(\nu'\nu'')e - \frac{E_\nu{}'}{k_B T}, \tag{4}$$

where ν is wavenumber and v' and v'' are the vibrational quantum number of the upper and lower states, respectively. In this method, $\Delta v = (v' - v'') = 0, -1, -2$. The vibrational temperature is calculated from the slope of a linear fit on the plot of Ln $(I\nu'\nu''/\nu^4 A(\nu'\nu''))$ as a function of E'_ν [13].

Moreover, the molecular dissociation degree is known as an important parameter for molecular gaseous plasmas. This parameter is used to study the processing of different industrial materials [14]. Molecular dissociation in plasma discharge media can significantly affect the plasma chemistry and thus critical plasma parameters, such as the electron energy distribution functions (EEDFs) and plasma electron number density. Many plasma models have the capability of predicting the dissociation degree. Thus, knowledge of the density of radicals resulting from the molecular dissociation in plasma discharge media is achievable. Generally, the nitrogen dissociation and its relation with the discharge parameters is studied via the monitoring of the optical emission ratio from the particular radiative levels of nitrogen and argon atomic species. Hence, the nitrogen dissociation can be written according to the following reactions [15]:

$$N_2(A^3\Sigma_u^+) + N(^4S) \rightarrow N_2(X^1\Sigma_g^+, 6 \leq v \leq 9) + N(^2P),$$

$$e + N_2(X^1\Sigma_g^+, v = 0) \rightarrow e + 2N(^4S),$$

$$e + N_2(X^1\Sigma_g^+, v = 0) \rightarrow e + N(^4S) + N(^2D).$$

It must be noted that, in the Ar/N_2 mixture plasma discharges, the population of the $N_2(C^3\Pi_u)$ excited state results from the internal energy transfer between the argon metastable state and the ground state of the nitrogen molecules [3]. The argon metastable states are $Ar_m^*(^3P_2, ^3P_0)$, where the subscript m stands for the metastable species, and their energies are between 11.55 and 11.72 eV. These energies are higher than the threshold excitation energy (11.1 eV) of the nitrogen molecule. Therefore, if argon is added to the nitrogen plasma, the emission intensities are significantly increased, and consequently the concentration of the active species can be observed. This is expected based on the Penning effect, as follows [4]:

$$N_2(X^1\Sigma_g^+) + Ar_m^*(^3P_2, ^3P_0) \rightarrow N_2(C^3\Pi_u) + Ar.$$

However, the radiative decays are able to emit characteristic photons of the (0–0) band of the second positive system based on the following relation [15]:

$$N_2(C^3\Pi_u, \nu' = 0) \rightarrow N_2(B^3\Pi_g, \nu'' = 0) + h\upsilon.$$

As a result, the emission intensity of the (0–0) band of the second positive system is proportional to the population density of the $N_2(C^3\Pi_u)$state [4]. Hence, the variation of the intensity ratio of N/N_2 shows the variations of dissociation degree along with the Ar II intensity. Moreover, it expresses the variations of high-energy electrons creating the Penning effect.

In this work, a comparative study is performed on the argon excitation and nitrogen vibrational temperatures in the plasma discharge medium of a manufactured RF plasma. The optical emission spectra of the plasma discharge medium are analyzed and the population densities of electrons in the atomic and molecular states in the plasma discharge medium of the plasma jet are obtained.

3. Results and discussion

By applying RF power to the plasma jet, as shown in Figure 1a, gas breakdown occurs. Therefore, charged particles such as electrons, ions, and neutral atoms and molecules in the ground and excited states are produced in the plasma discharge medium of the designed RF plasma jet. The neutral and ionized states in the gas atoms and molecules (here, atomic argon and molecular nitrogen) build up until they reach appreciable values and the Ar/N_2 gas mixture plasma species start to radiate at different wavelengths. Thus, to recognize the discharge species, the obtained spectra from the OES technique for the RF plasma jet and with different Ar/N_2 mixtures and input power of 48 W are analyzed. The obtained spectra are normalized with the responses and transmission curve of the spectrometer and optical fiber that are provided by the spectrometer manufacturer.

Figures 3a–3c show the significant emission peaks corresponding to the several transition lines of nitrogen and argon. The major emission lines represent the light emitted by N_2 molecules that are shown in Figures 3a and 3c and Ar atoms as seen in Figure 3b. In different Ar/N_2 gaseous mixtures, the dominant emission mainly originates from the excited molecular nitrogen in the wavelength range of 310–390 nm, as shown in Figure 3c. Furthermore, the emission lines with higher intensities in the discharge medium of the RF plasma jet are related to the argon emission lines (Ar I, 4p→4s, 650–890 nm), as depicted in Figure 3b, and the N_2 emission band ($C^3\Pi_u \rightarrow B^3\Pi_g$, 365–385 nm), as seen in Figure 3a. For Ar 4p→4s transitions, the radiated intensities peak at many wavelengths. These peaks mainly occur at 794.81 nm ($4p_1 \rightarrow 4s$), 801.47 nm ($4p_2 \rightarrow 4s_2$), 811.5 nm

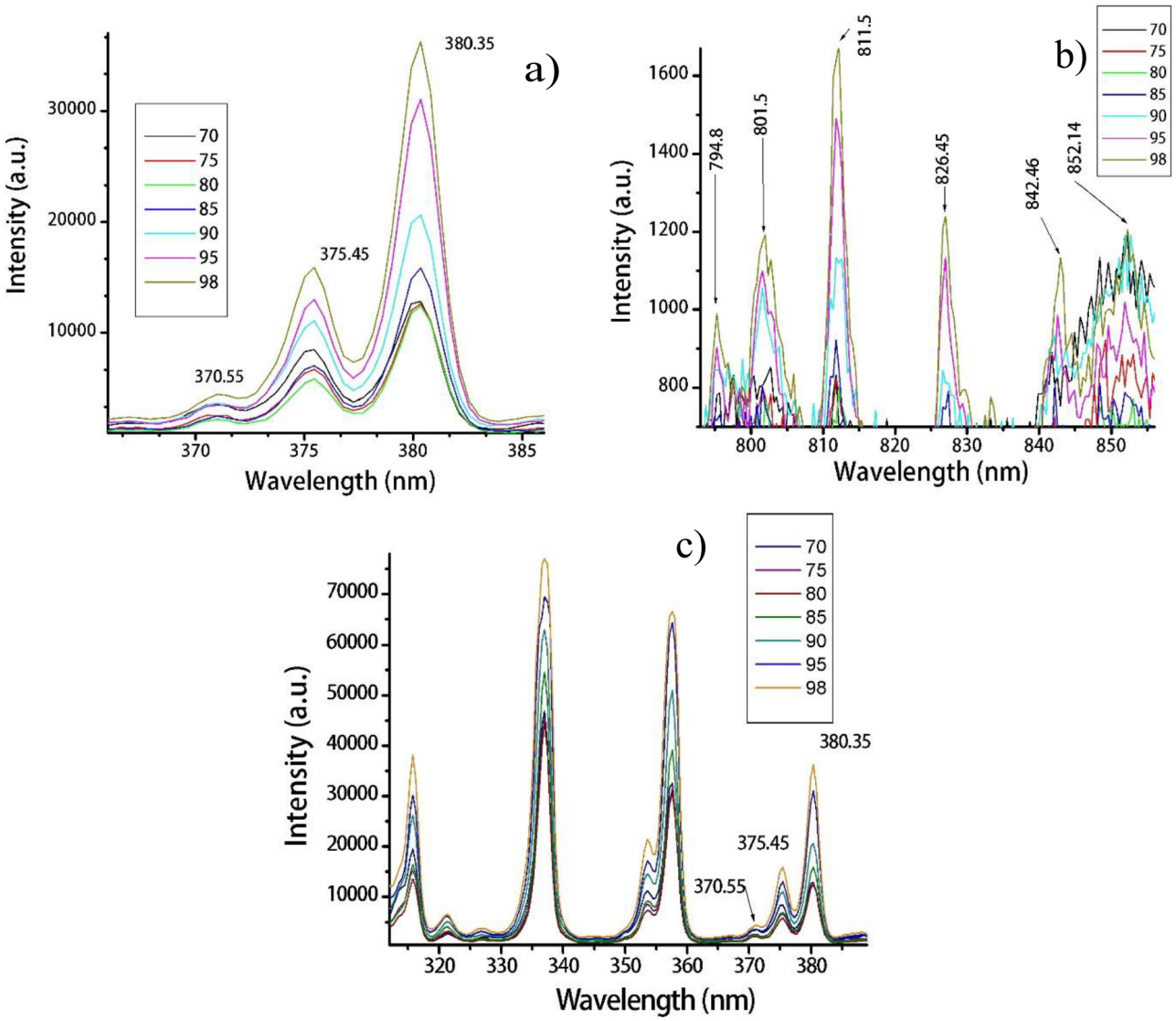

Figure 3. The obtained spectra from the developed RF plasma jet at the input power of 48 W for a) N_2 ($C^3\Pi_u \rightarrow B^3\Pi_g$) in the wavelength range of 370–385 nm, b) Ar I lines in the wavelength range of 794–853 nm, and c) N_2 ($C^3\Pi_u \rightarrow B^3\Pi_g$) in the wavelength range of 320–385 nm for different percentages of Ar in the Ar/N_2 gaseous mixture.

($4p_3 \rightarrow 4s_2$), 826.45 nm ($4p_1 \rightarrow 4s_1$), 842.46 nm ($4p_2 \rightarrow 4s_1$), and 852.1 nm ($4p_1 \rightarrow 4s_1$). The excitation $2p_1$ level of argon is known as one-step electron impact excitation from the ground state.

For the Ar/N_2 gaseous mixture plasma in the pressure of 50 mTorr, Lock et al. [16] obtained all the optical emission spectra in the wavelength range of 200–950 nm. The maximum intensity of the obtained spectra for the argon contribution of 70% and 90% was reported as 250 and 350 in arbitrary units (a.u.), respectively. It must be noted that the optical emission spectra line in the wavelength range of 200–900 nm was experimentally found. Moreover, the maximum intensity of the spectrum for 70% and 90% of argon in the Ar/N_2 mixture is 45,000 and 65,000 a.u., respectively. However, the observed difference between these findings and the results obtained by Lock et al. [16] for the wavelength range of 290–950 nm might be due to the operational Ar/N_2 gaseous mixture pressure, since the gas pressure in the performed experiments is kept at about 760 Torr. Using

the OES technique, Lock et al. [16] identified the excited species in the electron beam-generated plasma with argon, nitrogen, and their mixtures and the electron temperature was measured. Moreover, their system was vacuumed by a turbo pump with a base pressure of about 5×10^{-6} Torr.

To determine the excitation temperature, T_{exc}, from Eq. (1) and T_v from Eqs. (2) and (3) under the Boltzmann approximation, the neutral argon and excited nitrogen emission lines are obtained from the NIST database and listed in Table 1 [2]. Here, E_k and E_i are the energies of the upper and lower levels of the radiative transitions, respectively.

Influences of the argon contribution in the Ar/N_2 gaseous mixture on the spectral intensity of the RF plasma jet for Ar I, N_2, OH, and stronger UVC spectra at the wavelength of 247 nm (NO) are shown in Figures 4a–4f [17]. As is seen, the increase of the Ar percentage in the mixture, i.e. up to about 80%, results in the reduction of the emission intensity of all the excited atoms and molecules, as shown in Figures 4a, 4b, 4c, 4e, and 4f, except for NO molecules, as shown in Figure 4d. This might be due to the decreasing of the required energy for excitation of the argon atoms and nitrogen molecules and consequently the direct effects on the elastic and excitation cross-sections. From the argon contribution of about 80% onwards, due to the enhancement of argon and nitrogen ionization rates, the emission intensities start to increase once again. The spectroscopic features of RF plasma discharges with the Ar/N_2 mixture at the gas pressure of 0.1–0.5 mbar were studied by Khan et al. [15]. Their findings showed that there is a drastic enhancement in the emission intensity at 70% argon contribution in the Ar/N_2 mixture. Moreover, Lock et al. [16] showed that, at lower N_2 contributions in the Ar/N_2 mixture, while the intensity of the emitted spectra from the molecular nitrogen is linearly increased, the emitted spectra from atomic argon rapidly increase for argon contributions of 90% to 100% in the mixture. Figure 4e shows that the emission intensity of nitrogen smoothly increases at higher argon contributions. Thus, the EEDF tail expands towards the higher energies, since nitrogen excitation with the high-energy electrons is more probable. Moreover, the higher plasma electron number density results in larger dissociation rates for N_2. On the other hand, as seen in Figure 4f, the emission intensity from the Ar II line increases at higher Ar percentages in the mixture. Thus, the population density of the high-energy electrons is increased. Furthermore, at the higher Ar percentages, the probability of formation of metastable Ar increases. Hence, as seen in Figure 4b, it directly affects the production of $N_2(C^3\Pi_u)$.

Generally, in atomic and molecular phenomena, the electron collision cross-section is a fundamental quantity that characterizes each collision process among the energetic electrons and gaseous atomic and molecular particles. Figures 5a and 5b show the cross-section of the argon atom and nitrogen molecule as a function of the incident electrons' energy [18]. Generally, in plasma discharge media, the large excitation cross-sections would result in generation of metastable and radiative states. On the other hand, the elastic collisions are the only electron-cooling processes [16]. Thus, in this work, the elastic reactions have a critical role owing to the low energy of colliding electrons with the argon atoms and nitrogen molecules.

In the following, using Eqs. (1)–(4), both the atomic excitation and molecular nitrogen vibrational temperatures are calculated. As seen in Figure 6a, the slope of $\mathrm{Ln}(I\lambda_{ki}/A_{ki}g_k)$ determines the argon excitation temperature, T_{exc}. Moreover, the slope of $\mathrm{Ln}(N_2(\nu')/N_2(0))$ gives the nitrogen vibrational temperature, T_{vib}, as seen in Figure 6b.

On the other hand, based on Eqs. (1) and (3), the excitation and vibrational temperatures of both the atomic argon and molecular nitrogen are calculated at different Ar/N_2 mixtures and presented in Table 2.

It could be concluded that the increase of the argon contribution in the Ar/N_2 mixture rapidly influences

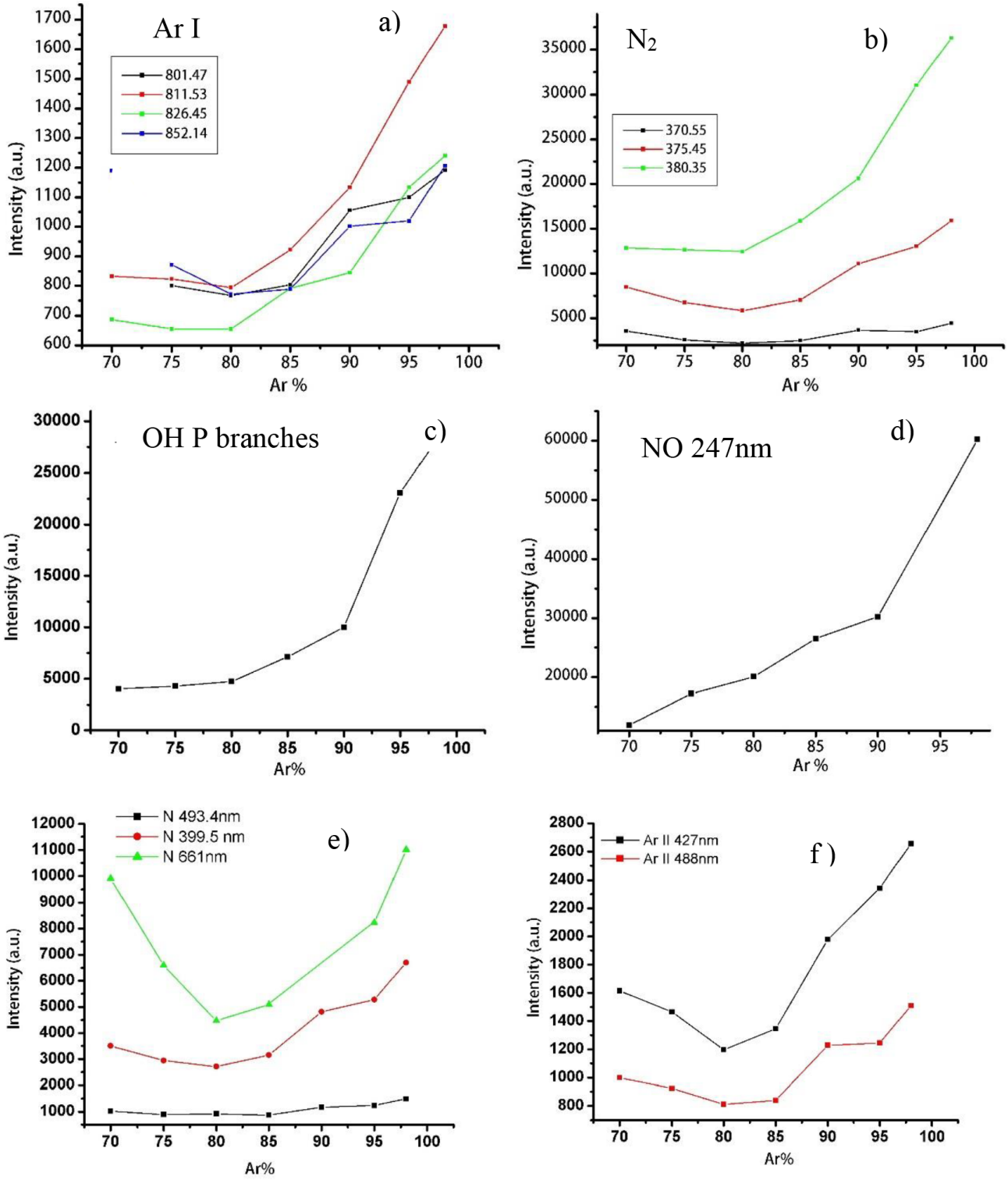

Figure 4. The spectral intensity of emission from a) argon atoms, b) nitrogen molecules, c) hydroxide molecules, d) UVC spectra peaks at the wavelength of 247 nm for the emission line of NO, e) neutral nitrogen atom, and f) excited argon atom versus the Ar percentages in the Ar/N_2 mixture.

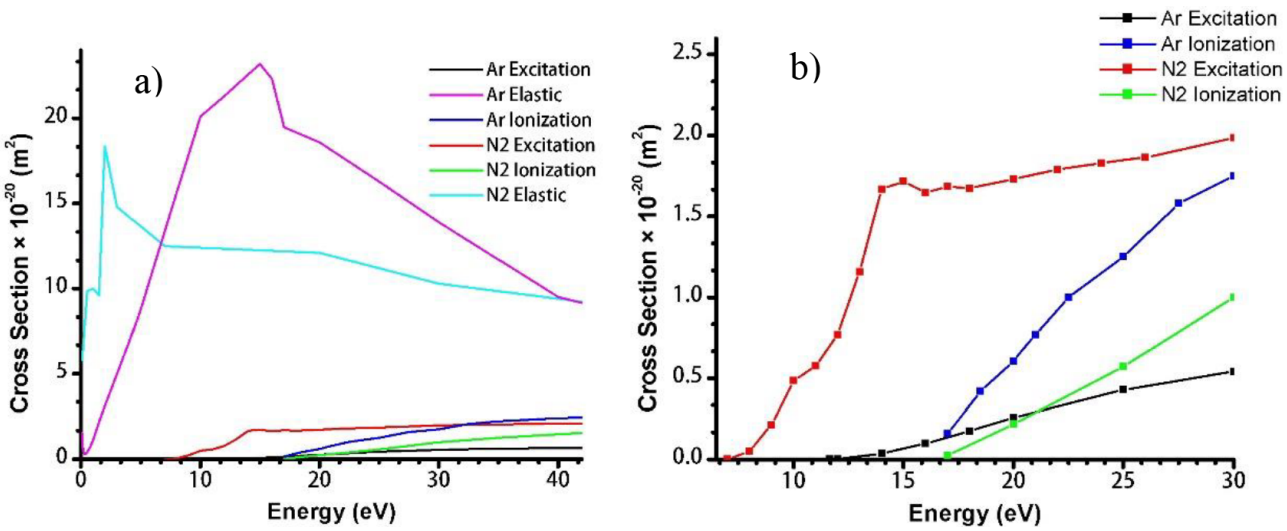

Figure 5. The excitation, ionization, and elastic collision cross-sections of atomic argon and molecular nitrogen versus the colliding electrons energy ranges as a) 0–30 eV and b) 6–30 eV [18].

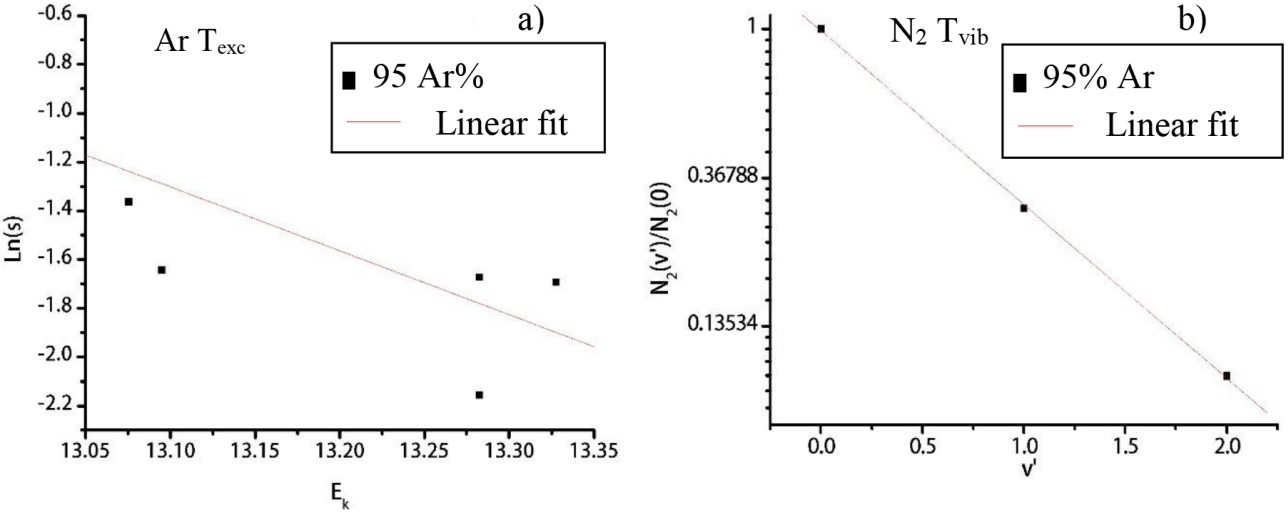

Figure 6. Boltzmann approximation plot for a) argon excitation temperature and b) nitrogen vibrational temperature of plasma electrons for Ar/N_2 containing 95% Ar and 5% N_2.

the emission intensities of the typical atomic and molecular spectra. At lower argon percentages in the Ar/N_2 mixture, the excitation and vibrational temperature are increased. This might be due to the drastic enhancement of the elastic collision cross-sections for the colliding electrons with argon atoms at electron energies of more than 5 eV. Moreover, when the argon amount in the Ar/N_2 mixture increases, the Penning excitation and dissociation of argon will increase the number density of excited states of N_2 and N_2^+ rather than those of argon ones.

Variations of the vibrational and excitation temperatures of the plasma discharge in the RF plasma jet in terms of argon contribution in the Ar/N_2 mixture are depicted in Figures 7a–7c. As is seen, increasing the argon contribution in the mixture results in the decreasing of the electrons' temperature. This must be due to the increasing of energy losses by the electrons during the elastic collision with N_2 molecules, since the elastic

Table 2. Excitation and vibrational temperatures in discharge medium of the developed RF plasma jet at the various percentages of Ar in the Ar/N_2 mixture.

Ar percentage in the Ar/N_2 mixture	T_{exc}(eV)	±5% error	T_V (eV), $\Delta v = -2$	±5% error	T_V (eV), v = 0, –1, –2	±5% error
70	2.07	0.104	0.34	0.017	0.35	0.018
75	0.56	0.028	0.28	0.014	0.29	0.014
80	0.42	0.021	0.26	0.013	0.27	0.013
85	0.42	0.021	0.24	0.012	0.26	0.013
90	0.40	0.020	0.26	0.013	0.28	0.012
95	0.38	0.019	0.21	0.010	0.23	0.018
98	0.38	0.019	0.22	0.011	0.24	0.014

cross-section for the atomic argon is greater than that of the molecular nitrogen for electron energies of about 10 eV. Moreover, the argon excitation temperature versus its percentage in the Ar/N_2 mixture, as shown in Figure 7a, is similar to the molecular nitrogen vibrational temperature, as depicted in Figures 7b and 7c. This is in agreement with the experimental findings of Ohata [19] on the evolution of temperature in a RF ICP jet by a 1500-W power supply. There, it was shown that the plasma temperature increases with the increase of the N_2 amount in the Ar/N_2 mixture. However, these observations will not collaborate the experimental results of Khan et al. [15] for 0.5 mbar and 150 W.

It must be noted that, since for dermatology applications, more nitrogen species with lower temperatures are required [20], the Ar/N_2 gaseous mixture with about 95% Ar and 5% N_2 would be the best gaseous mixture. Moreover, the most suitable spectral emission lines to study the relative concentrations of N and N_2 species are at the wavelength of 493.5 nm for N and the wavelength of 380.4 nm for N_2 due to their close excitation threshold energies of 13.2 eV and 11.1 eV, respectively. Figure 8 shows the spectral emission line intensity ratio of [N(493.5 nm)/N_2(380.4 nm)] as a function of argon contribution in the mixture [15]. As is shown, the intensity ratio is reduced at the higher argon contributions in the mixture. This might be due to the fact that, in the atmospheric pressure plasma discharges, the Penning effect is more effective than the other dissociation reactions.

4. Conclusions

In this work, the obtained optical emission spectra from the excited atomic Ar and molecular N_2 in a designed RF DBD plasma jet are analyzed and the argon excitation and nitrogen vibrational temperatures are calculated. The contribution of argon in the Ar/N_2 mixture is varied from 70% to 98%. The temperature of different formed species in the plasma discharge medium of the RF plasma jet are obtained. In the operational conditions of the RF plasma jet, the highest emission intensities for the neutral argon (Ar I) are recorded in the wavelength range of 790–850 nm. It was observed that, at the wavelength of 811.53 nm, the radiation intensity of Ar $4p \rightarrow 4s$ transitions at 98% argon presence in the Ar/N_2 mixture is higher than those of the other transitions. The emission intensity of the formed species inside the discharge medium of the RF plasma jet was increased at the higher argon contributions in the mixture and this resulted in the increase of the metastable particles' density. Furthermore, it was shown that the Penning effect is reduced at higher argon contributions. Thus, this directly affects the temperature of all of the formed species. Besides, it was shown that, at the lower Ar percentages in the mixture, both the argon excitation and the nitrogen vibrational temperatures are higher. It was found that, when the argon contribution in the mixture is about 85%, the plasma formed by the RF plasma

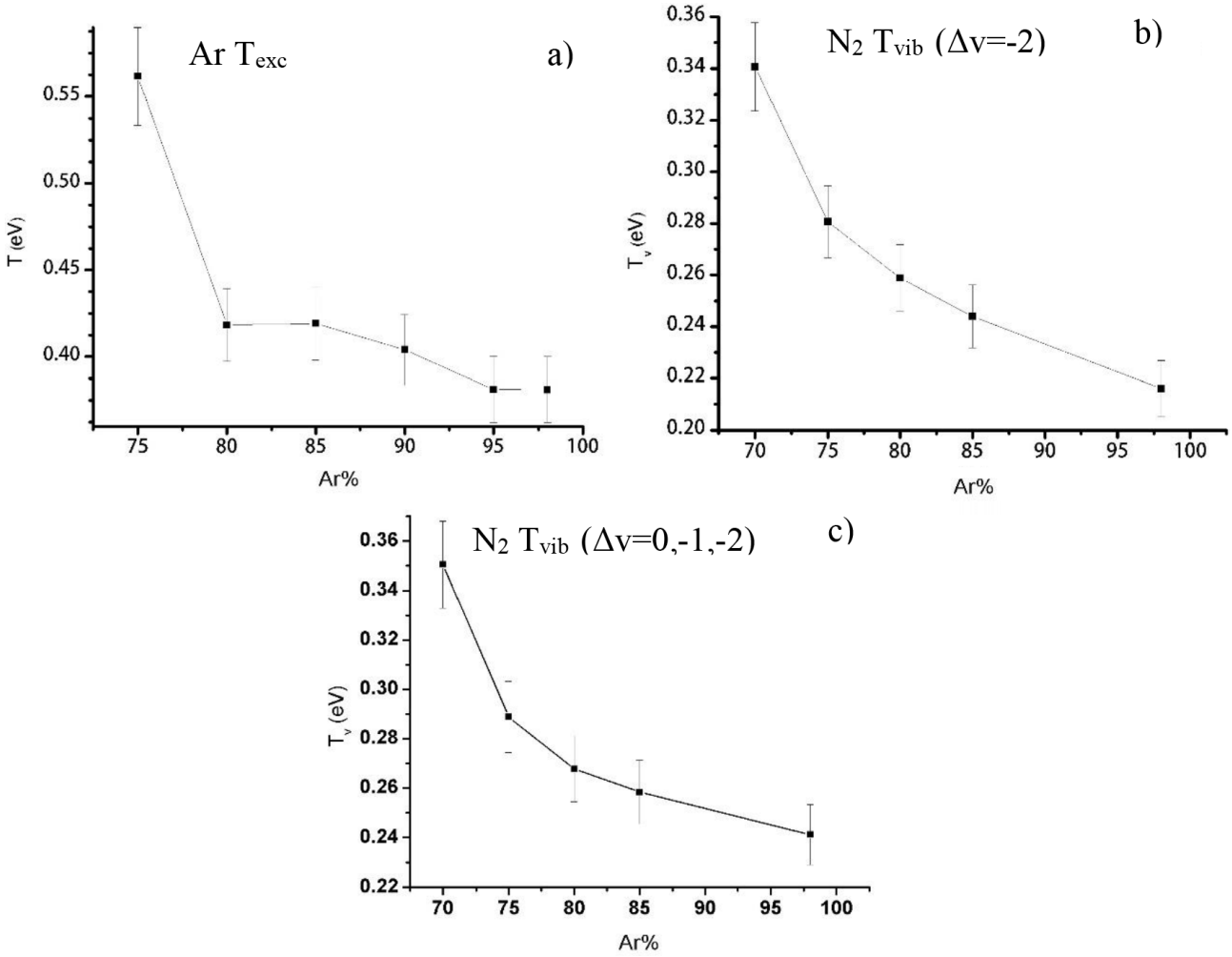

Figure 7. Variations of a) argon excitation and nitrogen vibrational temperatures of the plasma species versus the argon percentages in Ar/N_2 for b) $\Delta v = -2$ and c) $\Delta v = 0, -1$, and -2.

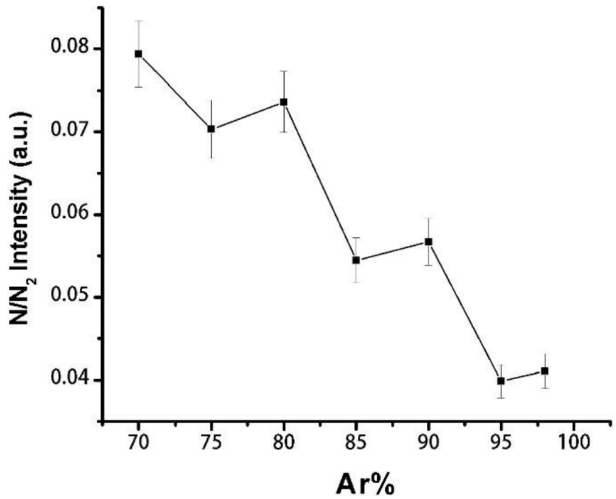

Figure 8. The spectral emission line intensity ratio of N/N_2 as a function of argon percentage in the Ar/N_2 gaseous mixture.

jet is most suitable for dermatology applications. This is due to the fact that, at lower argon percentages, the temperature of different formed species in the plasma discharge medium of the RF plasma jet will increase. It must be noted that, at the much higher argon contributions in the mixture, UVC radiation and excited atoms of argon are increased. Despite the suitability of UVC radiation for sterilization and dermatology applications, it can damage human skin.

Acknowledgment

We would like to acknowlege the Iran National Science Foundation (INSF) for financial supports within the project no. 91/S/23699.

References

[1] Foster, K. W.; Moy, R. L.; Fincher, E. F. *Journal of Cosmetic Dermatology* **2008**, *7*, 169-179.

[2] Florian, J.; Merbahi, N.; Wattieaux, G.; Plewa, J. M.; Yousfi, M. *IEEE T. Plasma Sci.* **2015**, *43*, 3332-3338.

[3] Cullen, P. J.; Milosavljević, V. *Prog. Theor. Exp. Phys.* **2015**, *2015*, 063J01.

[4] Qayyum, A.; Zeb, S.; Naveed, M. A.; Rehman, N. U.; Ghauri, S. A. *J. Quant. Spectrosc. Ra.* **2007**, *107*, 361-371.

[5] Doronin, Y. S.; Libin, M. Y.; Samovarov, V. N.; Vakula, V. L. arXiv:1107.3057, 2011.

[6] Zhang, X.; Zhang, X. F.; Li, H. P.; Wang, L. Y.; Zhang, C.; Xing, X. H.; Bao, C. Y. *Appl. Microbiol. Biot.* **2014**, *98*, 5387-5396.

[7] Laroussi, M. *IEEE T. Plasma Sci.* **2009**, *37*, 714-725.

[8] Babayan, S. E.; Jeong, J. Y.; Schütze, A.; Tu, V. J.; Moravej, M.; Selwyn G. S.; Hicks, R. F. *Plasma Sources Sci. T.* **2001**, *10*, 573-578.

[9] Weltmann, K. D.; Kindel, E.; Brandenburg, R.; Meyer, C.; Bussiahn, R.; Wilke, C.; Von Woedtke, T. *Contrib. Plasma Phys.* **2009**, *49*, 631-640.

[10] Pandhija, S.; Rai, A. K. *Appl. Phys. B-Lasers O.* **2009**, *94*, 545-552.

[11] Britun, N.; Gaillard, M.; Ricard, A.; Kim, Y. M.; Kim, K. S.; Han, J. G. *J. Phys. D Appl. Phys.* **2007**, *40*, 1022-1029.

[12] Henriques, J.; Tatarova, E.; Guerra, V.; Ferreira, C. M. *J. Appl. Phys.* **2002**, *91*, 5622-5631.

[13] Herzberg, G. *Molecular Spectra and Molecular Structure I: Spectra of Diatomic Molecules*; D. Van Nostrand: London, UK, 1950.

[14] Popa, S. D. *J. Phys. D Appl. Phys.* **1996**, *29*, 411-415.

[15] Khan, F. U.; Rehman, N. U.; Naseer, S.; Naveed, M. A.; Qayyum, A.; Khattak, N. A. D.; Zakaullah, M. *Eur. Phys. J. Appl. Phys.* **2009**, *45*, 11002p1-11002p8.

[16] Lock, E. H.; Fernsler, R. F.; Slinker, S.; Walton, S. G. *Experimental and Theoretical Estimation of Excited Species Generation in Pulsed Electron Beam-Generated Plasmas Produced in Pure Argon, Nitrogen, Oxygen, and Their Mixtures, No. NRL/MR/6750-11-9333*; Naval Research Laboratory: Washington, DC, USA, 2011.

[17] Boudam, M. K.; Moisan, M.; Saoudi, B.; Popovici, C.; Gherardi, N.; Massines, F. *J. Phys. D Appl. Phys.* **2006**, *39*, 3494-3507.

[18] Raju, G. G. *Gaseous Electronics: Tables, Atoms, and Molecules*; CRC Press: Boca Raton, FL, USA, 2011.

[19] Ohata, M. *Anal. Sci.* **2016**, *32*, 219-224.

[20] Heinlin, J.; Isbary, G.; Stolz, W.; Morfill, G.; Landthaler, M.; Shimizu, T.; Steffes, B.; Nosenko, T.; Zimmermann, J. L.; Karrer, S. *J. Euro. Acad. Dermatol.* **2011**, *25*, 1-11.